Electronic Supplementary Information

Competitive Coordination Aggregation for V-shaped [Co_3] and Disc-like [Co_7] Complexes: Synthesis, Magnetic Properties and Catechol Oxidase Activity

Tufan Singha Mahapatra,[a] Dipmalya Basak,[a] Santanu Chand,[a] Jeff Lengyel,[b] Michael Shatruk,[b] Valerio Bertolasi,[c] and Debashis Ray*[a]

[a]*Department of Chemistry, Indian Institute of Technology, Kharagpur 721 302, India*

Fax: (+91) 3222-82252; Tel: (+91) 3222-283324; E-mail: dray@chem.iitkgp.ernet.in

[b]*Department of Chemistry & Biochemistry, Florida State University, Tallahassee, FL 32306, United States*

[c]*Dipartimento di Scienze Chimiche e Farmaceutiche and Centro di Strutturistica Diffrattometrica, Università di Ferrara, via L. Borsari, 46, I44121 Ferrara, Italy.*

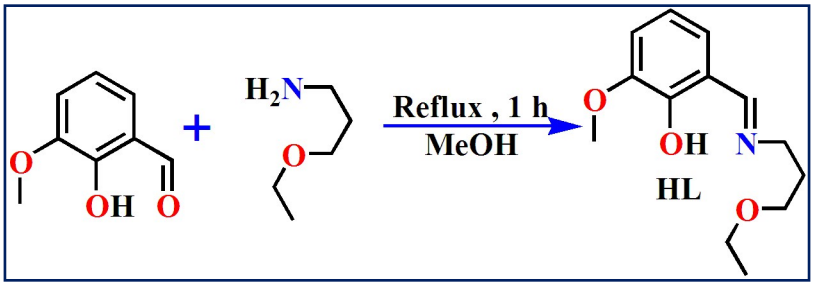

Scheme S1. Formation of HL

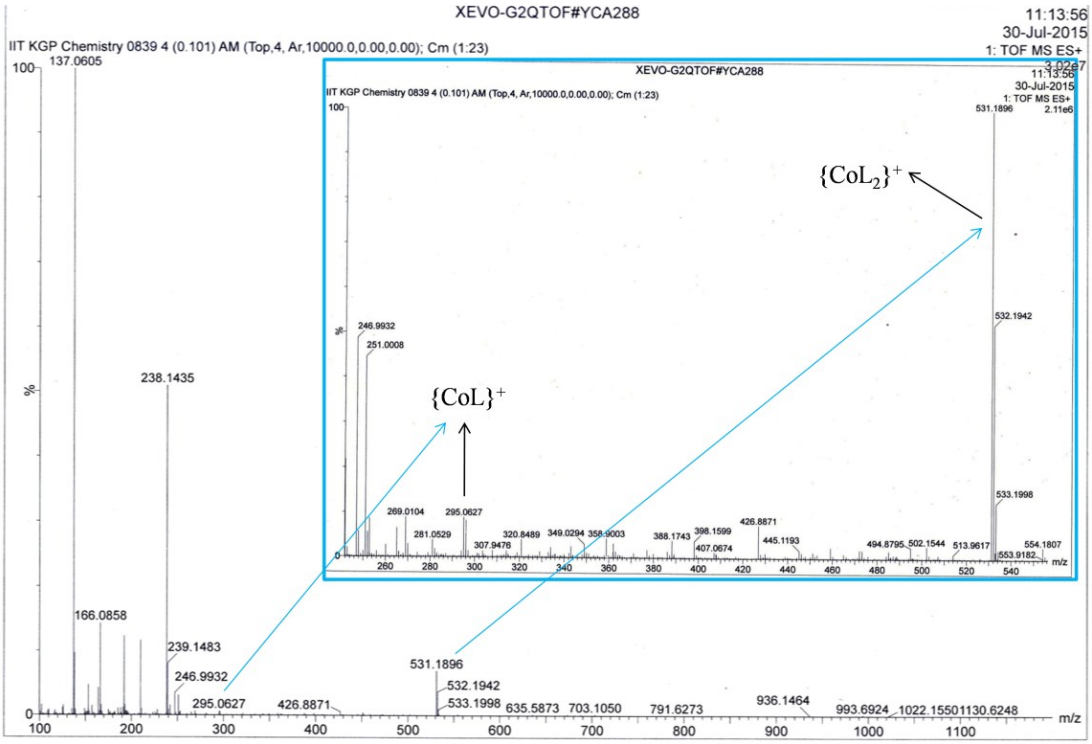

Fig. S1. Electrospray mass spectrum (ESI-MS positive) of **1** in MeOH solution

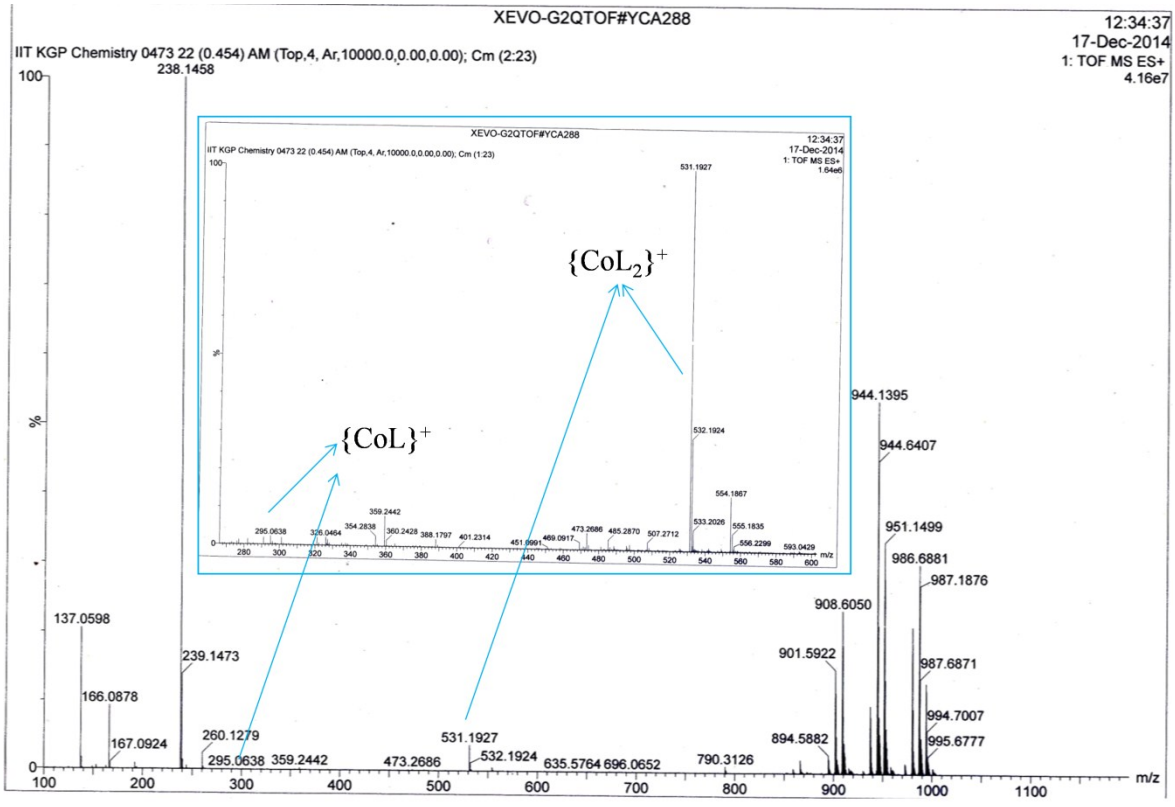

Fig. S2. Electrospray mass spectrum (ESI-MS positive) of **2** in MeOH solution

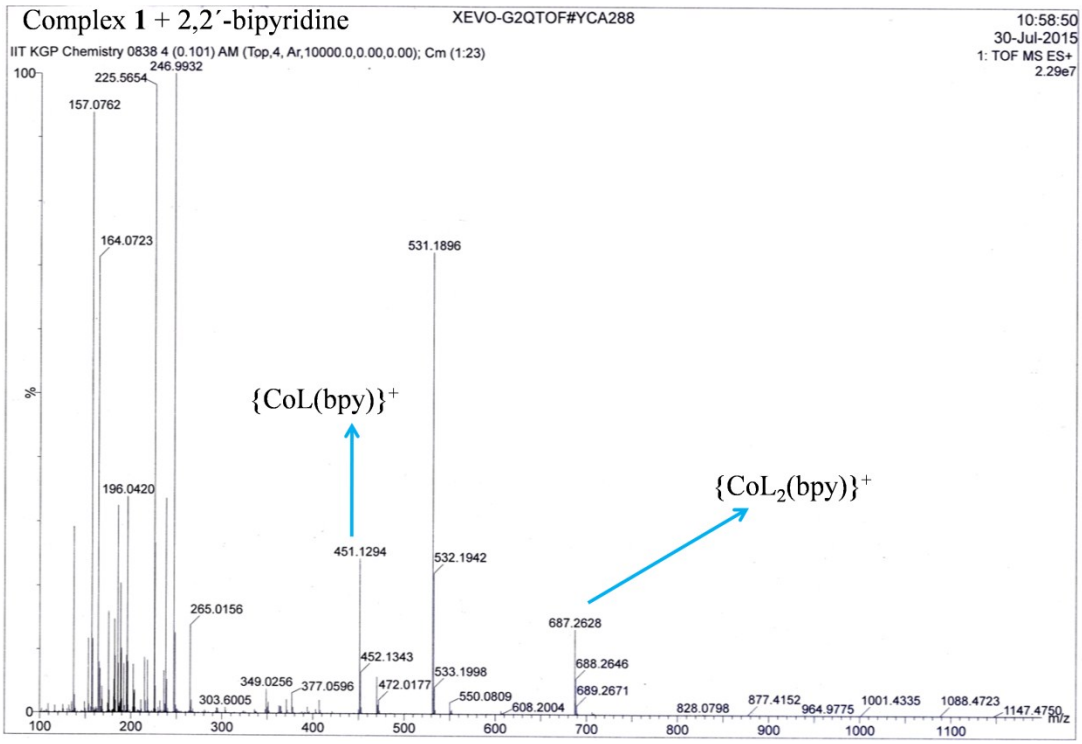

Fig. S3. Electrospray mass spectrum (ESI-MS positive) of **1** with 2,2′-bipyridine in 1:1 mole ratio in MeOH solution

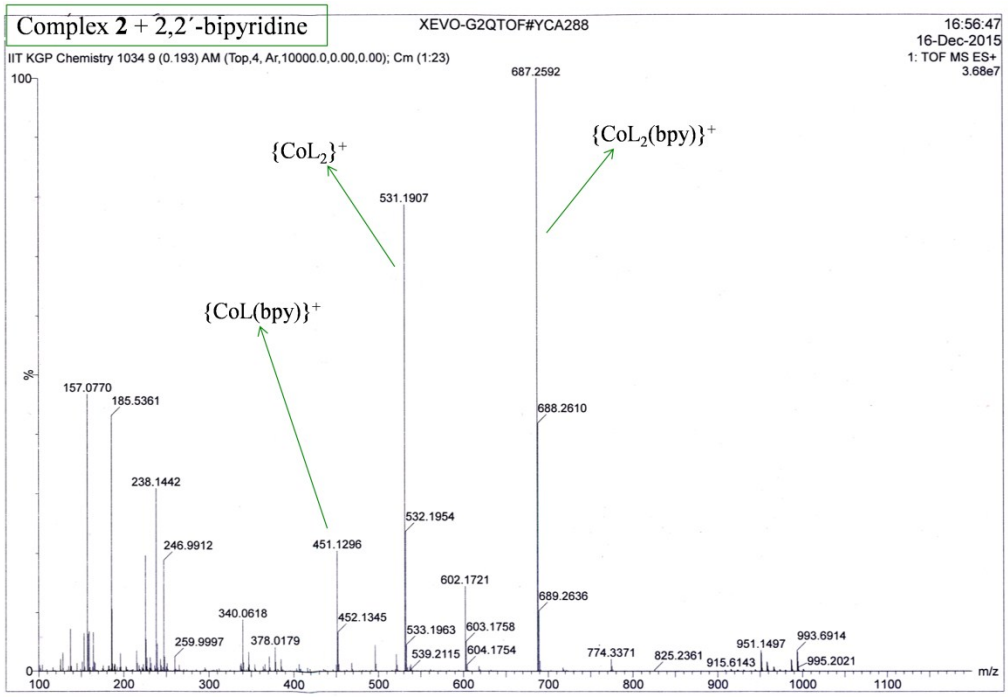

Fig. S4. Electrospray mass spectrum (ESI-MS positive) of **2** with 2,2′-bipyridine in 1:1 mole ratio in MeOH solution

$$\{CoL\} + 2\ bpy + 2\ NaClO_4 \longrightarrow [CoL(bpy)_2](ClO_4)_2 \quad ...(S1)$$

$$\{CoL_2\} + 2\ bpy + 2\ NaClO_4 \xrightarrow{-L} [CoL(bpy)_2](ClO_4)_2 \quad ...(S2)$$

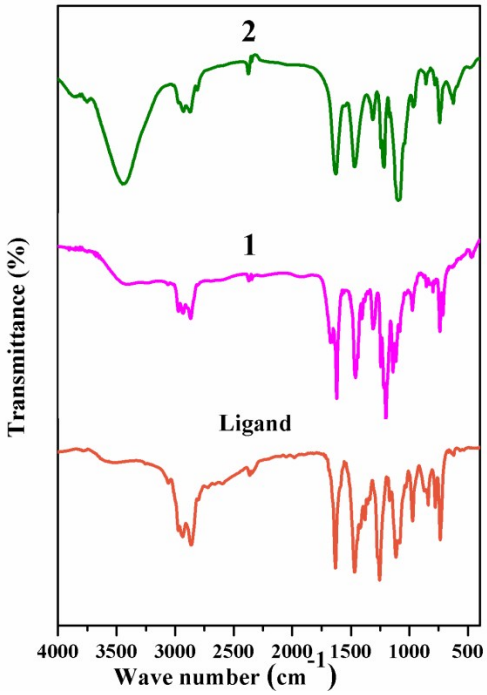

Fig. S5. FT-IR Spectra of the HL, **1** and **2**

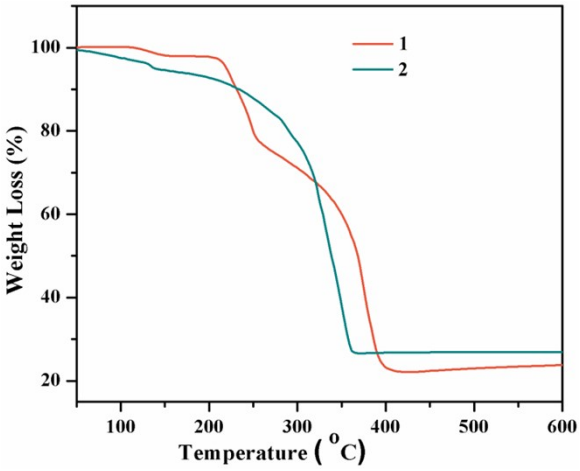

Fig. S6. Thermograms for **1**−**2** in air up to 600 °C

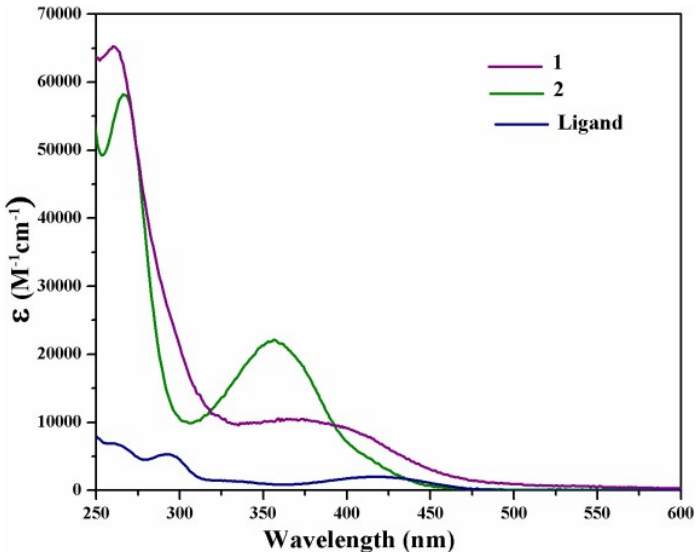

Fig. S7. Electronic spectra of the HL, **1** and **2** in MeOH

Table S1. Selected inter-atomic distances (Å) and angles (°) of **1**

Distances			
Co1-O5	1.986(3)	Co2-N3	2.082(4)
Co1-O15	2.066(3)	Co2-O4	2.305(4)
Co1-N1	2.099(4)	Co2-O11	2.309(3)
Co1-O1	2.110(3)	Co3-O12	1.990(3)
Co1-O4	2.135(4)	Co3-O17	2.078(3)
Co1-O3	2.234(3)	Co3-N4	2.092(4)
Co2-O8	1.989(3)	Co3-O8	2.111(3)
Co2-O1	1.989(3)	Co3-O11	2.120(4)
Co2-N2	2.061(4)	Co3-O10	2.215(3)
Angles			
O5-Co1-O15	176.30(13)	O1-Co2-O4	76.61(12)
O5-Co1-N1	86.85(15)	N2-Co2-O4	165.35(14)
O15-Co1-N1	90.86(15)	N3-Co2-O4	86.24(14)
O5-Co1-O1	86.75(12)	O8-Co2-O11	76.38(12)
O15-Co1-O1	95.00(12)	O1-Co2-O11	88.07(13)
N1-Co1-O1	168.18(14)	N2-Co2-O11	86.73(15)

O5-Co1-O4	94.19(14)	N3-Co2-O11	163.78(15)
O15-Co1-O4	89.37(15)	O4-Co2-O11	83.46(15)
N1-Co1-O4	112.36(15)	O12-Co3-O17	176.74(14)
O1-Co1-O4	78.03(12)	O12-Co3-N4	86.95(15)
O5-Co1-O3	88.48(13)	O17-Co3-N4	91.05(16)
O15-Co1-O3	88.91(13)	O12-Co3-O8	85.69(12)
N1-Co1-O3	96.69(14)	O17-Co3-O8	95.80(13)
O1-Co1-O3	73.21(12)	N4-Co3-O8	167.24(14)
O4-Co1-O3	150.91(13)	O12-Co3-O11	93.61(15)
O8-Co2-O1	160.75(12)	O17-Co3-O11	89.53(15)
O8-Co2-N2	98.06(14)	N4-Co3-O11	112.67(15)
O1-Co2-N2	92.23(14)	O8-Co3-O11	78.22(12)
O8-Co2-N3	91.20(15)	O12-Co3-O10	89.87(13)
O1-Co2-N3	101.70(14)	O17-Co3-O10	89.87(13)
N2-Co2-N3	105.56(15)	N4-Co3-O10	95.97(15)
O8-Co2-O4	90.20(13)	O8-Co3-O10	73.62(12)
Co1-O4-Co2	95.71(14)	O11-Co3-O10	151.28(14)
Co3-O11-Co2	95.85(13)	Co2-O8-Co3	106.72(12)
Co2-O1-Co1	106.92(13)		

Table S2 Bond-valence-sums for the cobalt atoms in **1**–**2**[a]

Complex **1**		
Atom	Co^{II}	Co^{III}
Co1	2.011	1.719
Co2	1.990	1.702
Co3	2.020	1.729
Complex **2**		
Co1	1.981	1.693
Co2	1.923	1.644

[a] The underlined values are the closest ones to the charge for which it was calculated; the nearest whole number can be considered as the oxidation state of that atom.

Table S3. Selected inter-atomic distances (Å) and angles (°) of **2**

Distances			
Co1-O1*	1.992(4)	Co1-O4	2.189(4)
Co1-O4*	2.054(4)	Co1-O2	2.298(5)
Co1-O1	2.059(4)	Co2-O4	2.110(4)
Co1-N1*	2.118(6)		
Angles			
O1*-Co1-O4*	111.12(18)	N1*-Co1-O4	163.8(2)
O1-Co1-O1*	163.14(10)	O1*-Co1-O2	95.13(19)
O4*-Co1-O1	79.4(17)	O4*-Co1-O2	152.68(17)
O1*-Co1-N1*	86.7(2)	O1-Co1-O2	73.32(17)
O4*-Co1-N1*	99.6(2)	N1*-Co1-O2	89.0(2)
O1-Co1-N1*	105.0(2)	O4-Co1-O2	96.66(19)
O1*-Co1-O4	77.71(17)	O4*-Co2-O4*	97.16(14)
O4-Co1-O4*	82.2(2)	O4-Co2-O4*	82.84(14)
O1-Co1-O4	91.21(18)	O4-Co2-O4#	180.0(3)

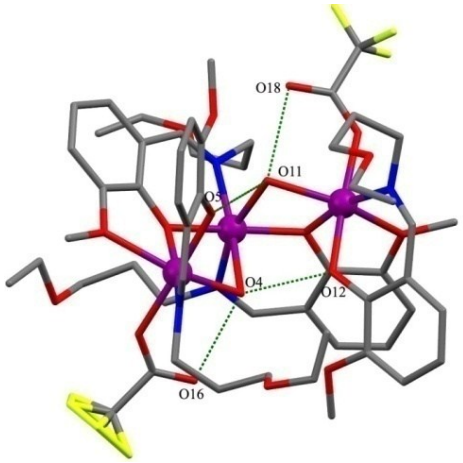

Fig. S8. Intramolecular hydrogen bonding connectivity in **1**

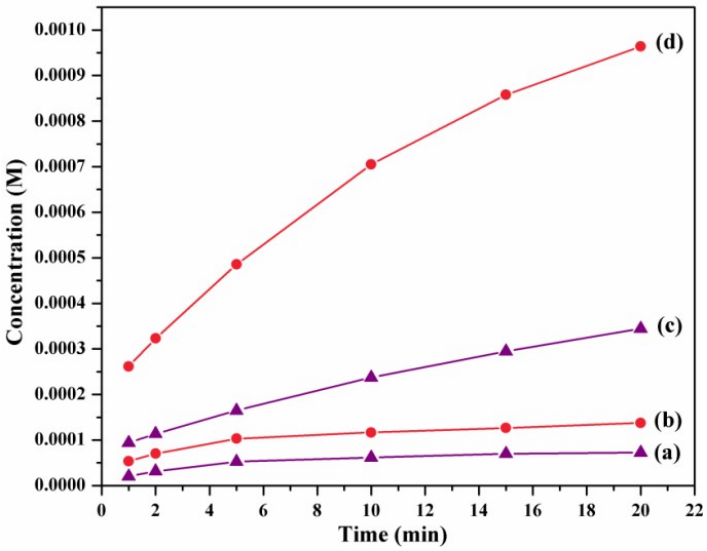

Fig. S9. Change in concentrations of H_2O_2 (a and b) and 3,5-DTBQ (c and d) during the catalytic reaction of 3,5-DTBCH_2 with **1** and **2**, respectively

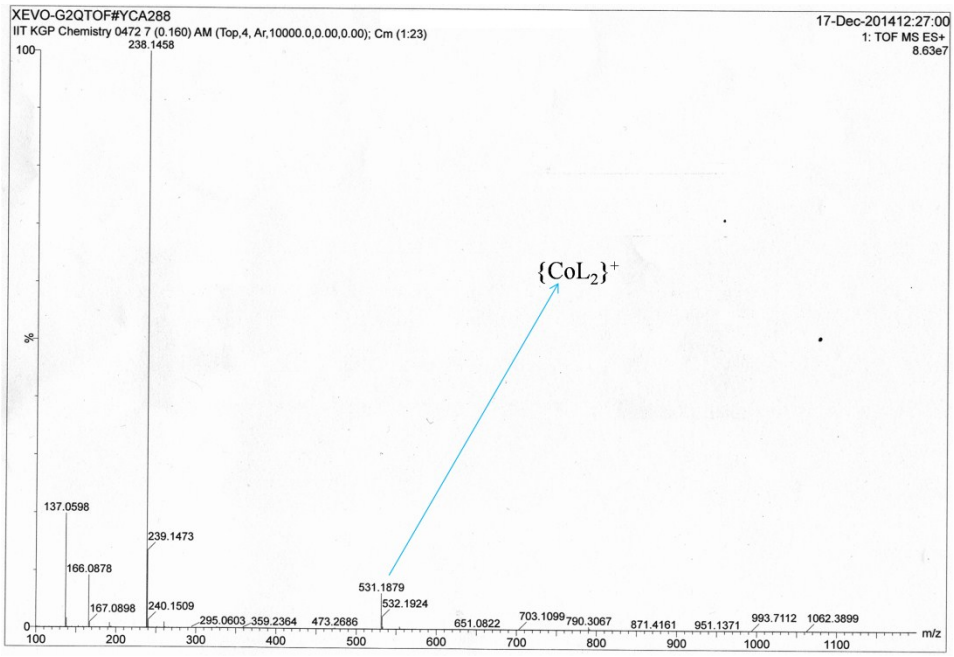

Fig. S10. Electrospray mass spectrum (ESI-MS positive) of **1** in MeCN solution

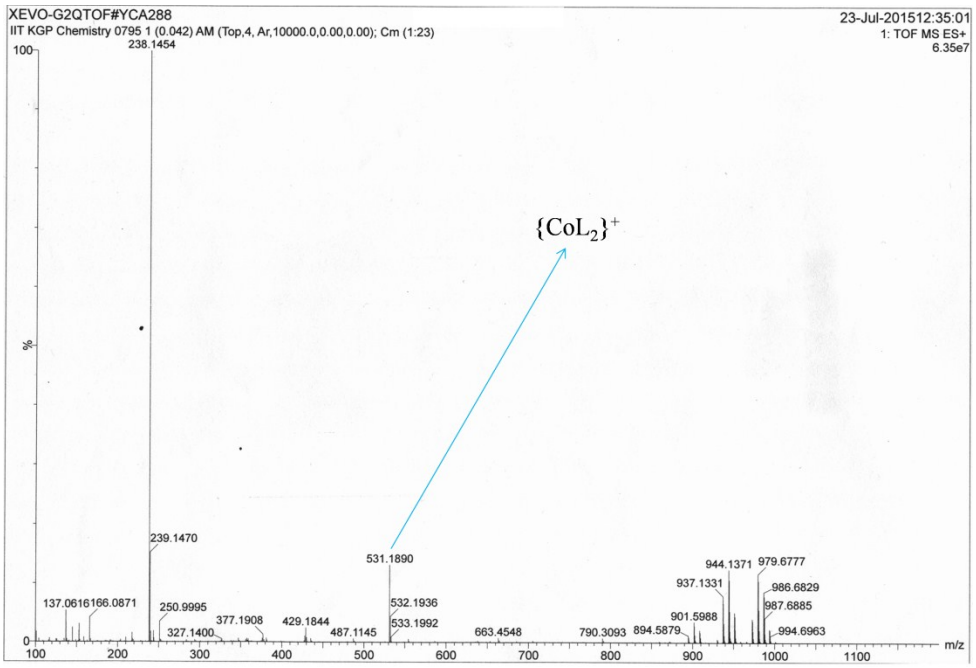

Fig. S11. Electrospray mass spectrum (ESI-MS positive) of **2** in MeCN solution

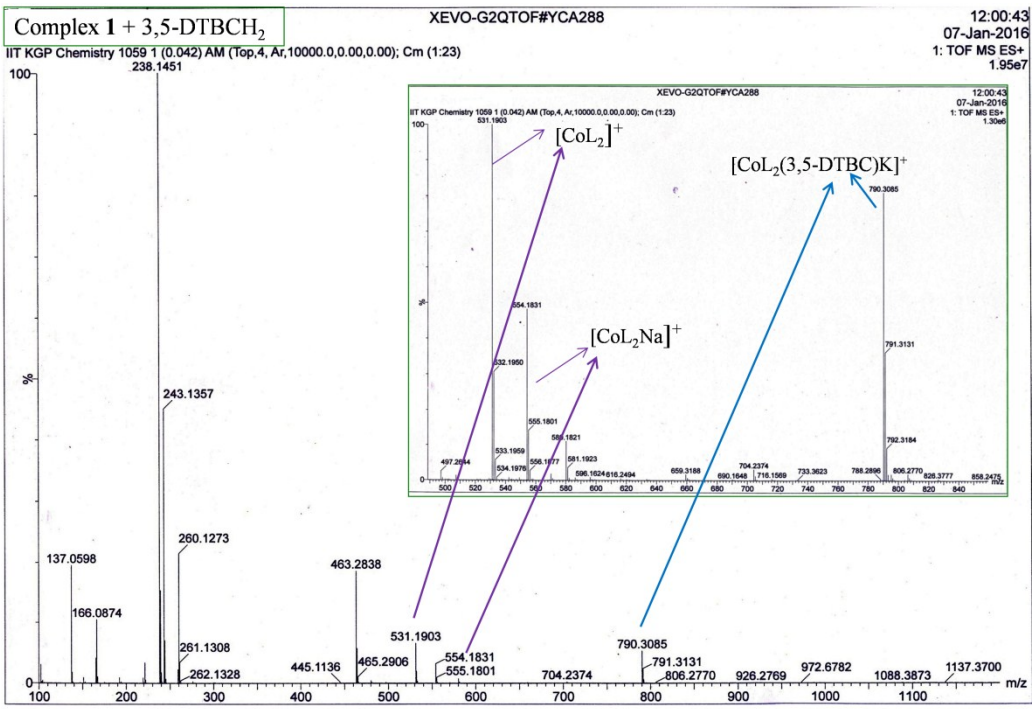

Fig. S12. Electrospray mass spectrum (ESI-MS positive) of **1** and 3,5-DTBCH$_2$ (1:100) in MeCN after 20 min of mixing

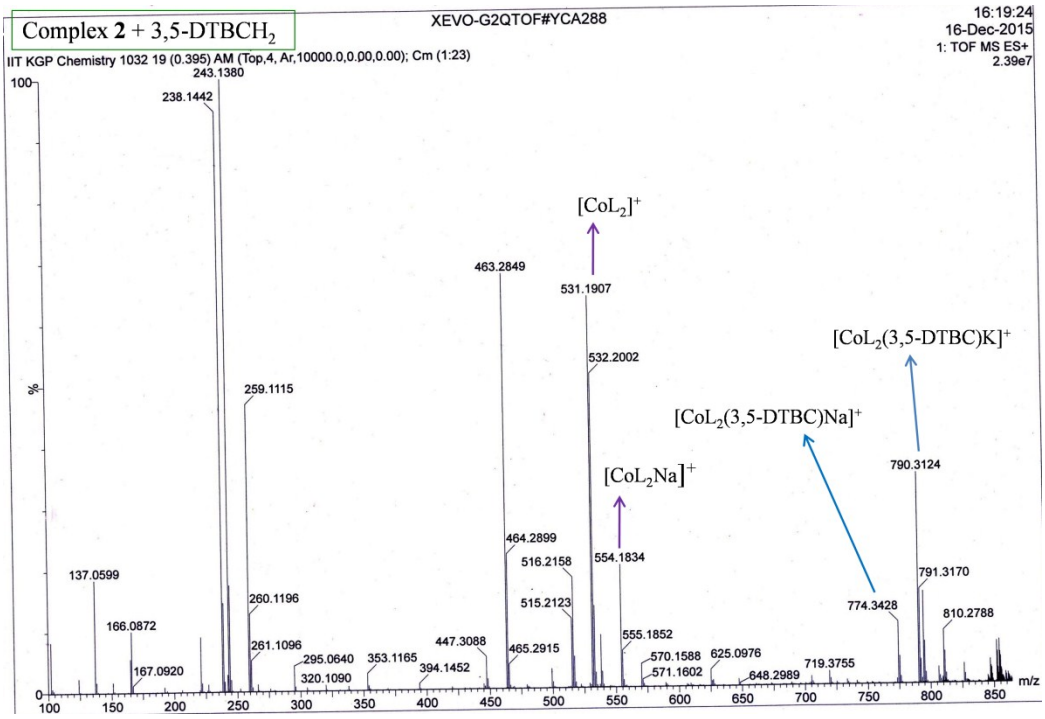

Fig. S13. Electrospray mass spectrum (ESI-MS positive) of **2** and 3,5-DTBCH$_2$ (1:100) in MeCN after 20 min of mixing

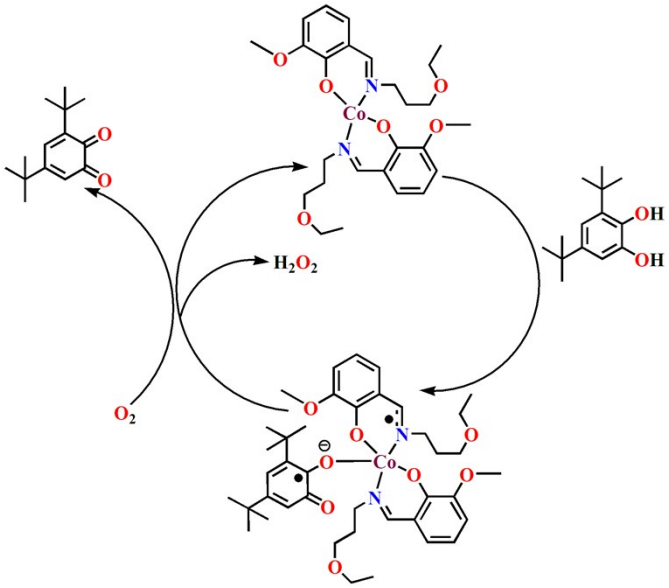

Scheme S2. Proposed mechanism for the catalytic cycle of 3,5-DTBCH$_2$ oxidation by Co(II) complexes.

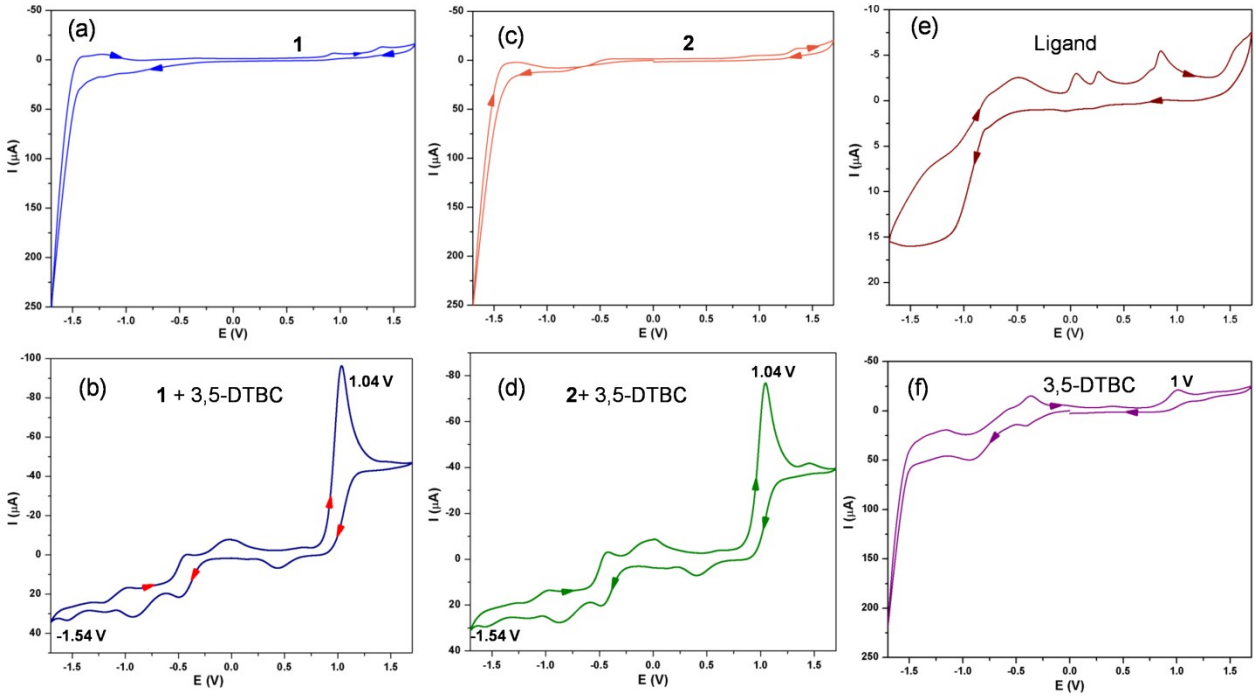

Fig. S14. Cyclic voltammogram of (a) **1** (10^{-4} M), (b) **1**+3,5 $DTBCH_2$ (10^{-2} M) (c) **2** (10^{-4} M), (d) **2**+3,5 $DTBCH_2$ (10^{-2} M), (e) ligand (10^{-3} M) and (f) 3,5 $DTBCH_2$ (10^{-3} M) in MeCN using 0.1 M $[^nBu_4][ClO_4]$ as the supporting electrolyte, a Pt disc working electrode and a Ag/AgCl reference electrode with scan rate at of 50 mV s^{-1}